2014 International Conference on Lightning Protection (ICLP), Shanghai, China

Wavelet Analysis of Chaotic Pulse Trains Prior To Subsequent Return Strokes in Malaysia

Chin-Leong Wooi, Zulkurnain Abdul-Malek, Noor Azlinda Ahmad, Mona Riza Mohd Esa, Zaini Zakaria
Institute of High Voltage and High Current (IVAT)
Faculty of Electrical Engineering, Universiti Teknologi Malaysia (UTM)
Johor Bahru, Malaysia
wooi5195@gmail.com, zulkurnain@utm.my, noorazlinda@utm.my, monariza@utm.my, ee_zai89@yahoo.com

Mohd Riduan Ahmad
Green Building, Massachusetts Institute of Technology (MIT), 02139 Cambridge, USA
mdriduan@mit.edu

***Abstract*—This paper presents a wavelet transformation of chaotic pulse trains (CPTs) prior to negative subsequent return strokes in Malaysia. A total of 593 recorded waveforms were examined. Even though several hundred waveforms were identified as containing CPTs, only 47 waveforms with CPTs preceding subsequent return stroke were selected for analysis. 19 samples are classified as CPTs associated with dart or dart-stepped leader (Type 1 CPTs) with spectral and spread regions average frequency range of 34.8-154.3 kHz and 56.2-81.4 kHz respectively. 28 samples are classified as chaotic pulse trains alone (Type 2 CPTs) with spectral and spread regions average frequency range of 24.6-121 kHz and 40.3-62 kHz, respectively. The Type 1 CPTs tends to radiate at a higher frequency range compared to Type 2 CPTs. The maximum power radiated by the largest pulse in Type 1 CPTs is more than six times larger than that for the Type 2 CPTs. In addition, the Type 1 CPTs have larger electric field variations, higher frequency, and higher power radiated spectrum compared to Type 2 CPTs. The reported radiated energy can be further compared with other lightning activities to give a better insight on the in-cloud breakdown processes prior to subsequent return strokes.**

Keywords-wavelet; chaotic pulse train; dart leader; dart-stepped leader; subsequent return stroke

I. INTRODUCTION

In most cases, chaotic pulse trains (CPTs) are often observed to precede natural subsequent return strokes (RSs) [1-7]. The first observation of chaotic pulse trains has been made by [1] in early eighties, where some of the observed subsequent return strokes were preceded by a train of pulses characterized by irregular shape, variable width and inconsistent inter pulse separation. Furthermore, two terms were introduced to describe the return strokes, namely the chaotic subsequent strokes, and the subsequent strokes preceded by chaotic leaders. In 2004, Gomes and coauthors [5] detail out the characteristic of these CPTs in detail and reported that the width of the individual pulse trains is in the range of a few microseconds, the lower limit of which may extend to sub-microsecond region. The pulse separation lies in the range of 2-20 μs and the most probable duration of the CPTs is 400-500 μs. 25% of the CPTs that these authors have observed occur before subsequent return stroke. In Guangdong province, authors [7] also perform broadband measurement on CPTs and they found that 48% of subsequent stroke were associated with CPTs while authors [6] with direct measurement found that 30% of subsequent stroke contain CPTs. Among these CPTs, some immediately preceded a subsequent stroke and continued up to the return stroke and the rest had a delay between the end of CPTs and the return stroke. This delay average value was 18 ms as claimed in [7] and 0.35 to 73 ms as claimed in [5].

On the other hand, CPTs are also found to be associated with cloud flashes other than ground flashes [4, 5, 8]. The authors in [4] have reported the occurrence of chaotic leader in intra-cloud (IC) flashes and in some cases it occurred with isolated breakdown pulses (IBPs), which suggest that perhaps chaotic leader associates with cloud activity rather than dart/dart stepped leader process. Because of this, the term chaotic pulse trains (CPTs) has been used rather than chaotic leader [5]. In this paper, we use the term chaotic pulse trains as defined by [5]. In recent research with the help of high speed camera [9-11] and VHF interferometer data [7], it is suggested that CPTs is a pulse activity associated with the dart phase of a subsequent leader discharge. However, detailed research on CPTs is currently not sufficient, in particular, studies on CPTs in tropical regions.

In previous years, Fourier Transform (FT) is the most popular method to transform the signal into frequency domain, mainly just focusing on the signal's spectral characterization. However, using the FT method one will not be able to preserve the time information which is very crucial in lightning research. Both temporal as well as spectral information can be kept intact by using the wavelet transformation. Sharma et al. [12] have used Derivative of Gaussian (DOG) wavelet algorithm to capture both the positive and negative peaks as separate waves and consequently the analysis of both the initial half and the overshoot of a bipolar pulse could be done. The usage of DOG

wavelet algorithm has been established earlier in lightning research by [13] to analyze the negative and positive return strokes in Brazil. Recent work by [14] had used Laplace wavelet algorithm to analyze the time–frequency characteristic of the first and subsequent return strokes. However, as suggested by [12], the DOG wavelet is the most stable so far because the much less divergence of the results compared to other algorithms including Laplace algorithm. Detailed explanation about DOG and Laplace theories and algorithms can be found in [12-15]. In this paper, we are motivated to study CPTs through the wavelet perspective or in time-frequency domain using the DOG wavelet algorithm.

II. METHODOLOGY

The lightning electric field measurements were performed in May 2015 within the monsoon period (May to September 2015) on the roof of a two-storey building (1°33'38.1"N 103°38'36.2"E) in Universiti Teknologi Malaysia's campus. UTM is located in the southern portion of peninsular Malaysia which is a tropical region. The electric field measuring system consists of a circular parallel plate antenna connected to an integrator and a unity-gain, high-input impedance amplifier. The configuration of the measuring system is shown in Figure 1. The antenna was connected to a Picoscope (Picoscope 5244B, 2 channel, 15-bit resolution (software resolution) with a sampling rate of 25 MSs^{-1} and 12.5 MSs^{-1}). The Picoscope was set to have 150 ms or 300 ms pre-trigger mode for total waveform of 500 ms or 1s, respectively. The setup is similar to experimental setups used in [16-21]. The criteria to identify the CPTs are similar to those in [5] where other than irregular in pulse shape, pulse width and pulse separation, pulse activity at beginning and at the end of pulse trains of amplitudes should be at least 10% of the maximum amplitude. However, only the largest peak of CPTs within window size of 200 μs had been taken for wavelet analysis in this study. The atmospheric sign convention is used throughout the paper, thus a negative return stroke (-CG) produces initially positive field changes. The distance was provided by Malaysia Meteorological Department (MMD) and all the electric field waveforms were normalized to 50 km to eliminate the dependency on distance. The triggering level was set to 1 V so that most of the lightning flash could be captured.

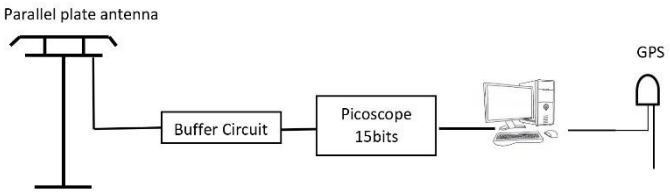

Figure 1. Schematic description of the fast electric field broadband antenna system.

III. WAVELET THEORY

Wavelet transforms were first used in geophysics research in the early 1980s for the analysis of seismic signals by Morlet [22, 23]. Since then, they have been used for numerous studies [24, 25]. A complete description of geophysical applications can be found in [24].

Wavelet analysis is based on an expansion of a signal in a space whose base can be orthogonal or non-orthogonal but finite functions. These functions are called wavelets. In the wavelet analysis, the wavelet term refer itself to a set of functions with limited waveform (non infinite) and which are expanded ($\psi(at)$) and translated ($\psi(t+b)$) versions of a wavelet, $\psi(t)$. The translated and expanded versions are called daughter wavelets, while $\psi(t)$ is the mother wavelet [13].

The continuous wavelet transform of a discrete sequence $x(t)$ is defined as the convolution of $x(t)$ with the daughter wavelets $\psi(t)$, given as [12] :

$$W_t(a,b) = \sum_{t=0}^{N-1} x(t)\psi * \left[\frac{(t-b)\delta t}{a}\right] \qquad (1)$$

where b is the translation parameter in time space and a is the dilation parameter.

IV. RESULT AND DISCUSSION

A total of 593 recorded waveforms were examined. Even though several hundred waveforms were identified as containing CPTs, only 47 waveforms with CPTs preceding subsequent return stroke were selected for analysis. The pulses were then wavelet-transformed using DOG algorithm. We have found the following common pulse characteristics, irrespective of the position of occurrence of CPTs. Each pulse trains consists of approximately more than 40 pulses with erratic amplitudes. The chaotic nature of the pulses especially with their erratic amplitudes makes it difficult to pinpoint the beginning and the end of each pulse with good accuracy. Therefore, this study focus on 200 μs window size with 100 μs before the largest pulse amplitudes and 100 μs after the largest pulse amplitudes in order to wavelet transform the waveform. It is discovered that the pulses with the largest amplitudes usually occur immediately after the initiation of the pulse trains.

Two types of chaotic pulse trains activity precede negative subsequent return stroke had been identified. Figure 2 shows CPTs which followed by easily identified dart leader or in some other cases this might be dart-stepped leader (Type 1 CPTs) before subsequent return stroke. Figure 3 shows only CPTs alone (Type 2 CPTs) without clear identified dart-stepped or dart leader before subsequent return stroke. 19 Type 1 CPTs and 28 Type 2 CPTs have been found out of 47 CPTs waveforms. The percentages are 40% and 60%, respectively and it is a bit different compared to 19% and 81% reported by [11]. Figure 4 (a)-(d) show example of negative return stroke preceded by CPTs in time domain (top) and its corresponding power spectrum in wavelet or time-frequency domain (bottom). The intensity level of the power spectrum is plotted according to color coding contour shown on the vertical colour bar on the right hand side of the bottom Figures 4(a)-(d). The spread region is bounded by the dark-red colour contour while the spectral region is bounded by the light-blue contour. Both spread and spectral regions definition are as explained in [15]. In this study, we found that there are some CPTs which are difficult to be

analyzed using wavelet analysis due to the reason that CPTs did not have a fix pattern and the frequency for the pulse trains may be different from case to case. Sometimes few spectral regions will appear in the power spectrum diagram as shown in Figure 4(a), but multiple spread regions seldom observed in the pulse trains signal because individual pulse with similar in peak amplitude and frequency seldom observed in this study.

Figure 4(a) shows the wavelet power spectrum of Type 1 CPTs from Figure 2, but due to the 200 µs window size limitation this figure did not show the clear dart-stepped or dart leader. Figure 4(b) shows the expand scale of Figure 4(a). It was observed that spectral and spread regions for Type 1 CPTs are approximately 85-336 kHz and 132-191 kHz, respectively. The maximum power radiated by Figure 2 (Type 1 CPTs) is about 1341 $(V/m)^2$ as shown in Figure 4(a) and 4(b). Figure 4(c) shows that the wavelet power spectrum Type 2 CPTs from Figure 3 without clear identified dart-stepped or dart leader. Figure 4(d) shows the expand scale of Figure 4(c) where the spectral and spread regions were roughly about 10-52 kHz and 20-25 kHz, respectively. The maximum power radiated by Figure 3 (Type 2 CPTs) is about 3300 $(V/m)^2$ as shown in Figure 4(c) and 4(d).

Table I presents the statistics of the wavelet power spectrum for these 2 type of CPTs events. The table shows the minimum, maximum and average values of the spectral and spread regions as well as peak energy (power peak) corresponding to two types of CPTs. The description of each terms used in Table 1 are as defined in [15, 26].

As tabulated in Table 1, it shows that the energy radiated by Type 1 CPTs is predominantly in the average spectral region from 34.8 to 154.3 kHz. Whereas, the average range of spread region is between 56.2 and 81.4 kHz. As can been seen from Table I, it is found that the Type 2 CPTs radiate energy predominantly from 24.6 to 121 kHz. Also, the average spread region of power radiated by the Type 2 CPTs is between 40.3 and 62 kHz. The maximum power radiated by the largest pulse in Type 2 CPTs is 4973 $(V/m)^2$. This is more than six times smaller compared to that for Type 1 CPTs which is 33,201 $(V/m)^2$. In addition, the average power spectrum of Type 1 CPTs is more than three times larger compared to Type 2 CPTs. When compared to Type 2 CPTs, the higher frequency range and higher radiated energy wavelet spectrum for Type 1 CPTs may be due to its larger electric field variations.

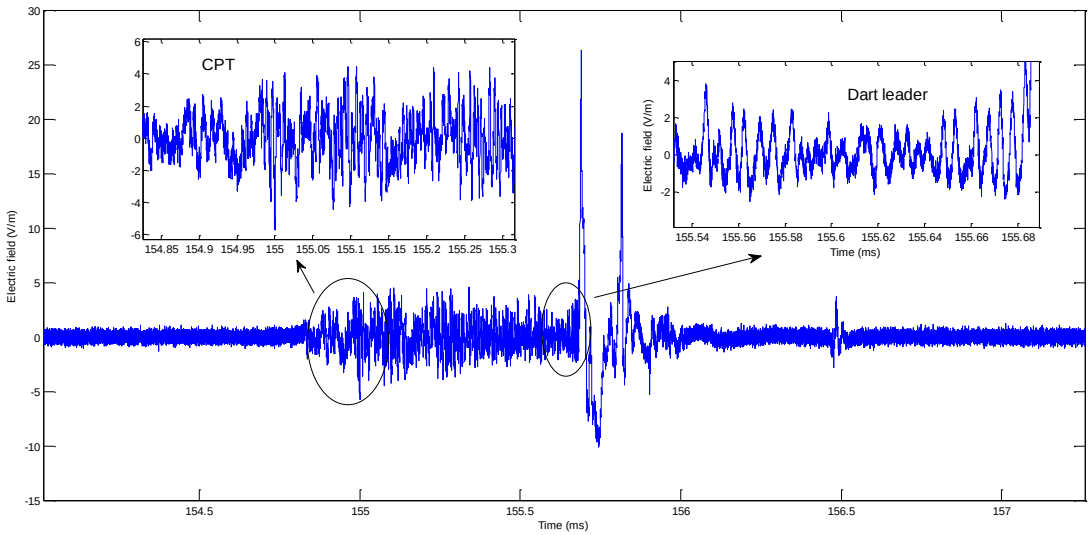

Figure 2. Chaotic pulse train was followed by dart leader (Type 1 CPTs) immediately before negative subsequent return stroke (flash number: 2015.05.01.191.155).

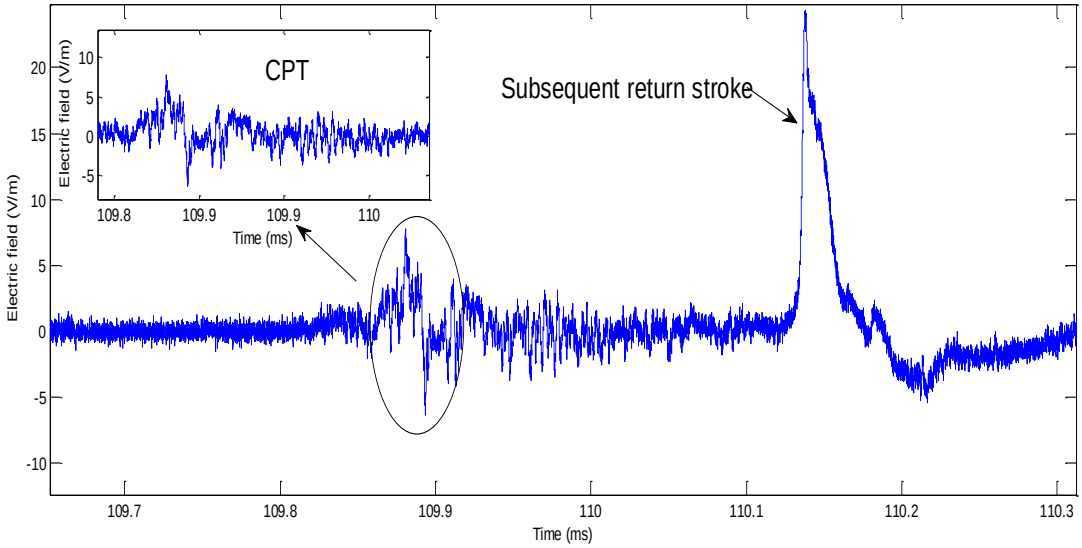

Figure 3. Chaotic pulse train activity alone (Type 2 CPTs) without any clear dart or dart-stepped leader before negative subsequent return stroke (flash number: 2015.05.01.157.109.934).

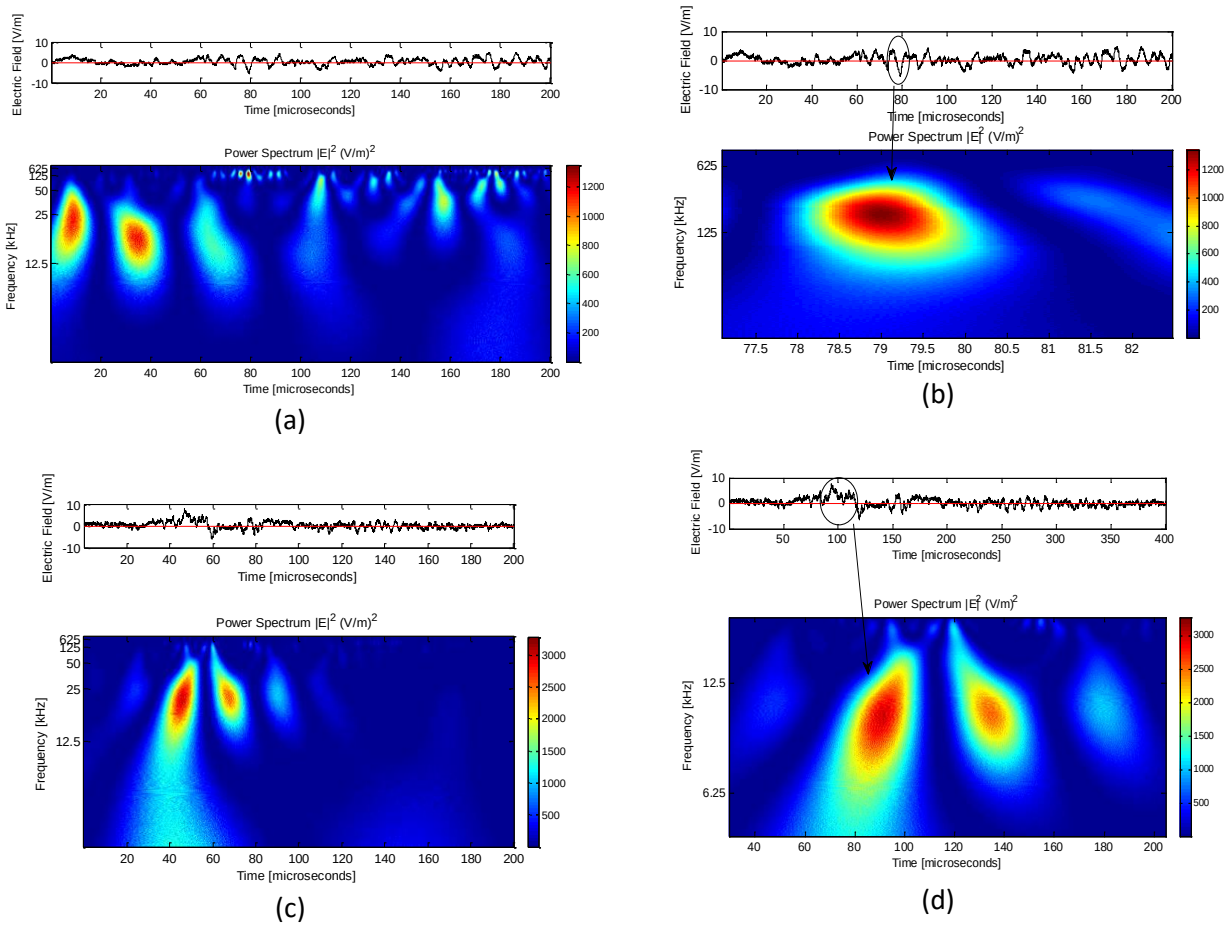

Figure 4. Wavelet power spectrum for (a) chaotic pulse trains with dart leader (flash number: 2015.05.01.191.155) (b) a part of chaotic pulse trains in 4(a) with dart leader in expanded scale (c) chaotic pulse trains alone (flash number: 2015.05.01.157.109.934) (d) a part of chaotic pulse trains alone in 4(c) in expanded scale.

TABLE I. STATISTICS OF WAVELET POWER SPECTRUM OF CPTS

Statistics (CPTs)	Type 1			Type 2		
	Spectral region (kHz)	*Spread region (kHz)*	*Power peak $(V/m)^2$*	*Spectral region (kHz)*	*Spread region (kHz)*	*Power peak $(V/m)^2$*
Minimum	3.2	5.8	106.5	2.2	4.7	40.7
Maximum	529.7	272.9	33201.9	762.2	408.5	4973.1
Average	34.8-154. 3	56.2-81.4	4241.1	24.6-121	40.3-62	1119.0
Standard deviation	42.7-155.3	60.6-83.7	9956.1	35.2-170.9	55.1-91.6	1299.6

V. CONCLUSION

To understand the temporal features of the frequency content of the different events of lightning, wavelet transform has been used in this study. Wavelet transformation has been done to 47 CPTs-preceded subsequent return strokes in order to understand the frequency and energy radiated by these pulse activities. Chaotic pulse trains were sometimes found to be associated with the dart leader or the dart-stepped leader (18 samples of Type 1 CPTs) and sometimes to be only chaotic pulse train alone (29 samples of Type 2 CPTs). The spectral and spread region average frequency ranges for Type 1 CPTs are 34.8-154.3 kHz and 56.2-81.4 kHz, respectively. The corresponding ranges for Type 2 CPTs are 24.6-121 kHz and 40.3-62 kHz, respectively. The maximum power radiated by the largest pulse in Type 2 CPTs is more than six times smaller than that for the Type 1 CPTs. While the average power spectrum of Type 1 CPTs is more than three times larger compared to Type 2 CPTs. Compared to Type 2 CPTs, the Type 1 CPTs also associated with dart leader or dart-stepped leader has a larger electric field variation thus a higher frequency range, and a higher energy wavelet spectrum. The power spectrum of other lightning activities can be compared with that for the CPTs in future studies to further understand the in-cloud breakdown processes that lead to return stroke activities.

ACKNOWLEDGMENT

Authors wish to thank Ministry of Science, Technology and Innovation, Ministry of Higher Education, and Universiti Teknologi Malaysia (Research Vote Nos. 4F672, 10H61 and 07H13) for the financial aid. The first author wish to thank Universiti Malaysia Perlis and Ministry of Higher Education for his postgraduate scholarship.

Mohd Riduan Ahmad is currently affiliated with Universiti Teknikal Malaysia Melaka (UTeM) and would like to acknowledge UTeM contributions in supporting his research at MIT.

REFERENCES

[1] C. D. Weidman, "The Submicrosecond Structure of Lightning Radiation Fields," University Microfilms International, 1982.

[2] J. Willett, J. Bailey, C. Leteinturier, and E. Krider, "Lightning electromagnetic radiation field spectra in the interval from 0.2 to 20 MHz," *Journal of Geophysical Research: Atmospheres (1984–2012)*, vol. 95, pp. 20367-20387, 1990.

[3] V. A. Rakov and M. A. Uman, "Waveforms of first and subsequent leaders in negative lightning flashes," *Journal of Geophysical Research: Atmospheres (1984–2012)*, vol. 95, pp. 16561-16577, 1990.

[4] S. M. Davis, *Properties of lightning discharges from multiple-station wideband electric field measurements*, 1999.

[5] C. Gomes, V. Cooray, M. Fernando, R. Montano, and U. Sonnadara, "Characteristics of chaotic pulse trains generated by lightning flashes," *Journal of Atmospheric and Solar-Terrestrial Physics*, vol. 66, pp. 1733-1743, 2004.

[6] J. Mäkelä, M. Edirisinghe, M. Fernando, R. Montaño, and V. Cooray, "HF radiation emitted by chaotic leader processes," *Journal of Atmospheric and Solar-Terrestrial Physics*, vol. 69, pp. 707-720, 2007.

[7] Y. Lan, Y. j. Zhang, W. s. Dong, W. t. Lu, H. y. Liu, and D. Zheng, "Broadband analysis of chaotic pulse trains generated by negative cloud‐to‐ground lightning discharge," *Journal of Geophysical Research: Atmospheres (1984–2012)*, vol. 116, 2011.

[8] M. R. Ahmad, M. Esa, D. Johari, M. M. Ismail, and V. Cooray, "Chaotic pulse train in cloud-to-ground and cloud flashes of tropical thunderstorms," in *Lightning Protection (ICLP), 2014 International Conference o*, 2014, pp. 808-809.

[9] M. Stolzenburg, T. C. Marshall, S. Karunarathne, N. Karunarathna, T. A. Warner, and R. E. Orville, "Stepped‐to‐dart leaders preceding lightning return strokes," *Journal of Geophysical Research: Atmospheres*, vol. 118, pp. 9845-9869, 2013.

[10] J. D. Hill, M. A. Uman, D. M. Jordan, J. R. Dwyer, and H. Rassoul, "“Chaotic” dart leaders in triggered lightning: Electric fields, X‐rays, and source locations," *Journal of Geophysical Research: Atmospheres (1984–2012)*, vol. 117, 2012.

[11] Y. Zhang, "Research on chaotic leader in cloud-to-ground lightning," presented at the XV International Conference on Atmospheric Electricity, 15-20 June 2014, Norman, Oklahoma, U.S.A., 2014.

[12] S. Sharma, V. Cooray, M. Fernando, and F. Miranda, "Temporal features of different lightning events revealed from wavelet transform," *Journal of Atmospheric and Solar-Terrestrial Physics*, vol. 73, pp. 507-515, 2011.

[13] F. Miranda, "Wavelet analysis of lightning return stroke," *Journal of Atmospheric and Solar-Terrestrial Physics*, vol. 70, pp. 1401-1407, 2008.

[14] Q. Li, K. Li, and X. Chen, "Research on lightning electromagnetic fields associated with first and subsequent return strokes based on Laplace wavelet," *Journal of Atmospheric and Solar-Terrestrial Physics*, vol. 93, pp. 1-10, 2013.

[15] M. R. M. Esa, M. R. Ahmad, and V. Cooray, "Wavelet analysis of the first electric field pulse of lightning flashes in Sweden," *Atmospheric research*, vol. 138, pp. 253-267, 2014.

[16] N. Azlinda Ahmad, M. Fernando, Z. A. Baharudin, V. Cooray, H. Ahmad, and Z. Abdul Malek, "Characteristics of narrow bipolar pulses observed in Malaysia," *Journal of Atmospheric and Solar-Terrestrial Physics*, vol. 72, pp. 534-540, 2010.

[17] C.-L. Wooi, Z. Abdul-Malek, N. A. Ahmad, and M. Mokhtari, "Characteristic of Preliminary Breakdown Preceding Negative Return Stroke in Malaysia," in *Energy Conversion (CENCON), 2015 IEEE Conference on*, 2015, pp. 348-353.
[18] C.-L. Wooi, Z. Abdul-Malek, N. A. Ahmad, M. Mokhtari, and B. Salimi, "Statistical Analysis on Preliminary Breakdown Pulses of Positive Cloud-to-Ground Lightning in Malaysia," *International Journal of Electrical and Computer Engineering (IJECE)*, vol. 6, pp. 844-850, 2016.
[19] C.-L. Wooi, Z. Abdul-Malek, B. Salimi, N. A. Ahmad, K. Mehranzamir, and S. Vahabi-Mashak, "A Comparative Study on the Positive Lightning Return Stroke Electric Fields in Different Meteorological Conditions," *Advances in Meteorology*, vol. 2015, p. 12, 2015.
[20] C.-L. Wooi, Z. Abdul-Malek, N.-A. Ahmad, and A. I. El Gayar, "Statistical analysis of electric field parameters for negative lightning in Malaysia," *Journal of Atmospheric and Solar-Terrestrial Physics*, vol. 146, pp. 69-80, 2016.
[21] B. Salimi, K. Mehranzamir, and Z. Abdul-Malek, "Statistical analysis of lightning electric field measured under Malaysian condition," *Asia-Pacific Journal of Atmospheric Sciences*, vol. 50, pp. 133-137, 2014.
[22] J. Morlet, G. Arens, E. Fourgeau, and D. Glard, "Wave propagation and sampling theory-Part I: Complex signal and scattering in multilayered media," *Geophysics*, vol. 47, pp. 203-221, 1982.
[23] J. Mot-let, G. Arensz, E. Fourgeau, and D. Giard, "Wave propagation and sampling theory-Part II: Sampling theory and complex waves," *Geophysics*, vol. 47, pp. 222-236, 1982.
[24] P. Kumar and E. Foufoula-Georgiou, "Wavelet analysis for geophysical applications," *Reviews of Geophysics*, vol. 35, pp. 385-412, 1997.
[25] C. Torrence and G. P. Compo, "A practical guide to wavelet analysis," *Bulletin of the American Meteorological society*, vol. 79, pp. 61-78, 1998.
[26] M. R. Mohd Esa, M. R. Ahmad, and V. Cooray, "Wavelet Analysis of the First Pulse of Initial Breakdown Process in Lightning Discharges," in *Progress in Electromagnetics Research Symposium (PIERS)*, 2013, pp. 1377-1380.